Journal of Applied Analysis and Computation
Volume 16, Number 6, December 2026, 3003–3028
Website:http://www.jaac-online.com
DOI:10.11948/20250197

NUMERICAL SOLUTIONS FOR PHASE-LAGGED VOLTERRA-FREDHOLM INTEGRAL EQUATIONS VIA SHIFTED LEGENDRE POLYNOMIALS

Mohamed E. Nasr[1,†], Sahar M. Abusalim[1] and Mohamed A. Abdel-Aty[2]

Abstract In this paper, a numerical method based on shifted Legendre polynomials combined with a least-squares formulation is developed for solving a class of phase-lagged Volterra–Fredholm integral equations of the second kind. Phase-lag effects arise naturally in many physical and engineering models involving delayed responses, leading to increased analytical and computational complexity. By employing shifted Legendre polynomials as basis functions, the proposed approach transforms the original integral equation into a system of algebraic equations that can be solved efficiently. Sufficient conditions for the existence and uniqueness of the solution are established using the Banach fixed-point theorem, and a convergence analysis of the proposed method is provided. Several numerical examples are presented to demonstrate the accuracy, stability, and efficiency of the method, including comparisons with existing approaches. The results confirm that the proposed scheme offers an effective and reliable tool for the numerical solution of phase-lagged Volterra–Fredholm integral equations.

Keywords Phase-lag, Volterra-Fredholm integral equations, Banach's fixed point, shifted Legendre polynomials, least squares method.

MSC(2010) 41A10, 65D15, 65F05.

1. Introduction

Integral equations play a crucial role in various branches of mathematics and arise naturally in many applications across science and engineering, including fluid mechanics [32], elasticity theory [11], thermoplastic plates [19], biology [33], and engineering [7]. Among these, Volterra–Fredholm integral equations (V–FIEs) are particularly significant due to their ability to model systems involving both memory effects and spatial interactions. Their theoretical and numerical analysis is closely related to functional analysis [3] and operator theory [1], and they have been successfully applied in electrodynamics and electromagnetic theory [36], population dynamics [38], and mathematical economics [13].

Because analytical solutions of V–FIEs are generally available only for special cases, extensive research has been devoted to the development of efficient numerical methods for approximat-

[†]The corresponding author.
[1]Department of Mathematics, College of Science, Jouf University, Sakaka 72388, Saudi Arabia
[2]Department of Mathematics and Computer Science, Faculty of Science, Benha University, Benha 13518, Egypt
Emails: menasr@ju.edu.sa(M. E. Nasr), sabosalem@ju.edu.sa(S. M. Abusalim), mohammed.abdallah@fsc.bu.edu.eg(M. Abdel-Aty)

ing their solutions. Existing approaches include Toeplitz matrix method [30] and Levin-type methods [20], Adomian decomposition techniques [24], modified Taylor series methods [25], polynomial-based approaches such as Lucas polynomials [23], Chebyshev collocation and spectral methods [21], quadrature rules [15], operational matrix techniques [10], and hat functions [27]. More recent studies have focused on nonlinear and fractional integral and integro–differential equations of the third kind, where spectral and cardinal-function-based schemes have demonstrated high accuracy and computational efficiency [8, 9, 18]. Block-based numerical strategies have also been introduced for nonlinear Volterra integral equations [4], while numerical methods have been extended to mixed and multidimensional Volterra–Fredholm formulations [5, 26]. Classical polynomial-based collocation techniques, such as the Legendre collocation method, continue to serve as a fundamental foundation for modern numerical schemes due to their accuracy and stability properties [31].

In many practical applications, system responses are not instantaneous but occur with a delay, leading naturally to phase-lag effects. Such phenomena arise in thermal conduction with memory, viscoelastic materials, signal processing with delayed feedback, wave propagation, and control systems. Incorporating phase-lag effects into integral equation models yields more realistic mathematical descriptions of these processes, but also introduces additional analytical and numerical challenges, particularly for nonlinear and mixed Volterra–Fredholm operators.

Despite these advances, many existing numerical methods remain tailored to specific kernel structures, discretization strategies, or restricted problem classes, which may limit their flexibility when solving phase-lagged Volterra–Fredholm integral equations. Motivated by this observation, the present work develops a unified numerical framework based on shifted Legendre polynomials combined with a least-squares formulation. By exploiting the orthogonality and favorable approximation properties of the shifted Legendre basis, the proposed method provides a stable and efficient approach for solving phase-lagged Volterra–Fredholm integral equations.

In this article, we consider a class of V-FIEs of the form:

$$\eta\Psi(u,t) = y(u,t) + \mu \int_0^t \int_0^1 G(t,\tau)k(u,v)\Psi(v,\tau)\mathrm{d}v\mathrm{d}\tau + \mu \int_0^t U(t,\tau)\Psi(u,\tau)\mathrm{d}\tau, \tag{1.1}$$

where $\eta \neq 0$ is a constant and μ is a parameter with various physical interpretations. The function $y(u,t)$ is given and continuous, while the unknown solution $\Psi(u,t)$ is sought in the product space $L_2[0,1] \times C[0,T]$, where $u \in [0,1]$ denotes the spatial variable and $t \in [0,T]$, with $T < 1$, represents time. The temporal kernels $G(t,\tau)$ and $U(t,\tau)$ are assumed to be continuous on $[0,T] \times [0,T]$, and the spatial kernel $k(u,v)$ belongs to $L_2([0,1] \times [0,1])$.

Phase-lag Volterra–Fredholm integral equations are often used to represent delays in physical processes, like how heat moves slowly, the way materials stretch and compress, and how signals are affected by delays in feedback In these kinds of systems, the response depends on both the current input and the past states, which creates a real-time lag. The analysis of phase-lag effects therefore requires careful examination of the kernel functions and their properties. Spectral analysis and asymptotic expansions are two common ways to find phase shifts in the frequency domain. A phase lag shows up as a shift between input and output that depends on the frequency. Taking these considerations into account, and following the passage of a shock wave, the resulting model leads to a Volterra–Fredholm integral equation of the second kind incorporating a phase-lag effect, given by

$$\eta\Psi(u,t+\delta t) = y(u,t+\delta t) + \mu \int_0^{t+\delta t} \int_0^1 G(t+\delta t,\tau)k(u,v)\Psi(v,\tau)\mathrm{d}v\mathrm{d}\tau$$

$$+\mu\int_0^{t+\delta t}U(t+\delta t,\tau)\Psi(u,\tau)\mathrm{d}\tau,\quad 0<\delta t<1, \tag{1.2}$$

under initial condition,

$$\Psi(u,0)=y(u,0)/\eta, \tag{1.3}$$

where δt represents the phase-lag parameter. Phase-lag refers to the delay in time between two related phenomena, typically associated with periodic or cyclical processes. It is commonly encountered in various fields, including physics [12], engineering [22], wave propagation [2], signal processing [14], and control systems [29].

When we apply Taylor expansion to the equation (1.2), omitting the second derivative, we obtain

$$\begin{aligned}\eta\Psi(u,t)+\eta\delta t\frac{\partial\Psi(u,t)}{\partial t}=&\,y(u,t)+\delta t\frac{\partial y(u,t)}{\partial t}\\&+\mu\int_0^{t+\delta t}\int_0^1\left(G(t,\tau)+\delta t\frac{\partial G(t,\tau)}{\partial t}\right)k(u,v)\Psi(v,\tau)\mathrm{d}v\mathrm{d}\tau\\&+\mu\int_0^{t+\delta t}\left(U(t,\tau)+\delta t\frac{\partial U(t,\tau)}{\partial t}\right)\Psi(u,\tau)\mathrm{d}\tau.\end{aligned} \tag{1.4}$$

Using initial condition (1.3) and integrating equation (1.4) with respect to time t, we obtain

$$\begin{aligned}\Psi(u,t)=&\,Y(u,t)-\frac{1}{\delta t}\int_0^t\Psi(u,x)\mathrm{d}x\\&+\frac{\mu}{\eta\delta t}\int_0^t\int_0^{x+\delta t}\int_0^1\left(G(x,\tau)+\delta t\frac{\partial G(x,\tau)}{\partial x}\right)k(u,v)\Psi(v,\tau)\mathrm{d}v\mathrm{d}\tau\mathrm{d}x\\&+\frac{\mu}{\eta\delta t}\int_0^t\int_0^{x+\delta t}\left(U(x,\tau)+\delta t\frac{\partial U(x,\tau)}{\partial x}\right)\Psi(u,\tau)\mathrm{d}\tau\mathrm{d}x,\end{aligned} \tag{1.5}$$

where

$$Y(u,t)=\frac{1}{\eta}[y(u,t)+\frac{1}{\delta t}\int_0^t y(u,x)\mathrm{d}x].$$

Using the triangular domain and the alternating order of integration, we obtain the following relationship:

$$\begin{aligned}\Psi(u,t)=&\,Y(u,t)-\frac{1}{\delta t}\int_0^t\Psi(u,\tau)\mathrm{d}\tau\\&+\frac{\mu}{\eta\delta t}\int_0^{t+\delta t}\int_0^1\Delta_1(t,\tau)k(u,v)\Psi(v,\tau)\mathrm{d}v\mathrm{d}\tau+\frac{\mu}{\eta\delta t}\int_0^{\delta t}\int_0^1\Delta_2(\tau)k(u,v)\Psi(v,\tau)\mathrm{d}v\mathrm{d}\tau\\&+\frac{\mu}{\eta\delta t}\int_0^{t+\delta t}\Xi_1(t,\tau)\Psi(u,\tau)\mathrm{d}\tau+\frac{\mu}{\eta\delta t}\int_0^{\delta t}\Xi_2(\tau)\Psi(u,\tau)\mathrm{d}\tau,\end{aligned} \tag{1.6}$$

where

$$\Delta_1(t,\tau)=\int_{\tau-\delta t}^t\left(G(x,\tau)+\delta t\frac{\partial G(x,\tau)}{\partial x}\right)\mathrm{d}x,\qquad \Delta_2(\tau)=\int_0^{\tau-\delta t}\left(G(x,\tau)+\delta t\frac{\partial G(x,\tau)}{\partial x}\right)\mathrm{d}x,$$

$$\Xi_1(t,\tau)=\int_{\tau-\delta t}^t\left(U(x,\tau)+\delta t\frac{\partial U(x,\tau)}{\partial x}\right)\mathrm{d}x,\qquad \Xi_2(\tau)=\int_0^{\tau-\delta t}\left(U(x,\tau)+\delta t\frac{\partial U(x,\tau)}{\partial x}\right)\mathrm{d}x.$$

The equation (1.6) is called the Volterra-Fredholm integral equation with a phase lag and is equivalent to equation (1.2)under condition (1.3).

The remainder of this article is organized as follows: The existence and unique solution of V-FIE with a phase lag are presented in Section 2. Section 3 introduces the system of Fredholm integral equations and derives the corresponding convergence analysis. In Section 4, shifted Legendre polynomials (SLPs) and their properties are given. Section 5 details the application of SLPs integrated with the least squares method (LSM) to transform the integral equation into a solvable algebraic system. The convergence analysis of the presented method is studied in Section 6. Section 7 provides the numerical results that show the accuracy and efficiency of the proposed technique. Finally, concluding remarks followed by a discussion of future research directions are provided in Section 8.

2. The existence and unique solution of equation (1.6)

In this section, the Banach fixed point theorem will be utilized to show that the solution to equation (1.6) exists and is unique. To facilitate this analysis, we reformulate equation (1.6) as the following integral operator:

$$\overline{V}\Psi = Y(u,t) + V\Psi, \tag{2.1}$$

where

$$\begin{aligned}
&V\Psi = V_1\Psi + V_2\Psi + V_3\Psi + V_4\Psi + V_5\Psi, \quad V_1\Psi = \frac{-1}{\eta}\int_0^t \Psi(u,\tau)\mathrm{d}\tau,\\
&V_2\Psi = \frac{\mu}{\eta\delta t}\int_0^{t+\delta t}\int_0^1 \Delta_1(t,\tau)k(u,v)\Psi(v,\tau)\mathrm{d}v\mathrm{d}\tau, \quad V_3\Psi = \frac{\mu}{\eta\delta t}\int_0^{\delta t}\int_0^1 \Delta_2(\tau)k(u,v)\Psi(v,\tau)\mathrm{d}v\mathrm{d}\tau,\\
&V_4\Psi = \frac{\mu}{\eta\delta t}\int_0^{t+\delta t} \Xi_1(t,\tau)\Psi(u,\tau)\mathrm{d}\tau, \quad \text{and} \quad V_5\Psi = \frac{\mu}{\eta\delta t}\int_0^{\delta t} \Xi_2(\tau)\Psi(u,\tau)\mathrm{d}\tau.
\end{aligned} \tag{2.2}$$

We assume the following:

(i) The kernel of position $k(u,v)\in L_2([0,1]\times[0,1])$, $u,v\in[0,1]$ satisfies $\left[\int_0^1\int_0^1 |k(u,v)|^2\mathrm{d}u\mathrm{d}v\right]^{\frac{1}{2}} \leq A$, A is a constant.

(ii) The functions $G(t,\tau)$, $U(t,\tau)$, and their partial derivatives are continuous in $C[0,T]$.

(iii) The functions $\Delta_1(t,\tau)$, $\Delta_2(\tau)$, $\Xi_1(t,\tau)$ and $\Xi_2(\tau)$ are continuous in $C[0,T]$ and satisfy the conditions $|\Delta_1(t,\tau)| \leq D_1$, $|\Delta_2(\tau)| \leq D_2$, $\Xi_1(t,\tau) \leq D_3$ and $\Xi_2(\tau) \leq D_4$ $\forall\, t,\tau \in [0,T]$, $0 \leq \tau \leq t \leq T < 1$, where D_1, D_2, D_3, D_4 are constants.

(iv) We define the norm on the space $L_2[0,1]\times C[0,T]$ as

$$\|\Psi(u,t)\| = \max_{0<t\leq T}\int_0^t \left[\int_0^1 \Psi^2(u,\tau)\mathrm{d}u\right]^{\frac{1}{2}}\mathrm{d}\tau.$$

We further assume that the given function $Y(u,t)$ satisfies $\|Y(u,t)\| \leq A_1$, A_1 is a constant.

Theorem 2.1. *If the conditions (i)–(iv) are satisfied, then equation (1.6) has a unique solution* $\Psi(u,t)$ *in the Banach space* $L_2[0,1]\times C[0,T]$, $0 \leq T < 1$, *under the condition*

$$|\mu| < \frac{|\eta|(\delta t - T)}{(D_1A + D_3)T + (D_1A + D_2A + D_3 + D_4)\delta t}, \quad 0 < \delta t < 1. \tag{2.3}$$

Proof. First, for normality, we utilize formula (2.2) to obtain

$$\begin{aligned}\|V\Psi\| &\leq \|V_1\Psi\| + \|V_2\Psi\| + \|V_3\Psi\| + \|V_4\Psi\| + \|V_5\Psi\| \\ &\leq \left|\frac{-1}{\delta t}\right| \left\| \int_0^t \Psi(u,\tau)\mathrm{d}\tau \right\| + \left|\frac{\mu}{\eta\delta t}\right| \left\| \int_0^{t+\delta t} \int_0^1 \Delta_1(t,\tau)k(u,v)\Psi(v,\tau)\mathrm{d}v\mathrm{d}\tau \right\| \\ &+ \left|\frac{\mu}{\eta\delta t}\right| \left\| \int_0^{\delta t} \int_0^1 \Delta_2(\tau)k(u,v)\Psi(v,\tau)\mathrm{d}v\mathrm{d}\tau \right\| + \left|\frac{\mu}{\eta\delta t}\right| \left\| \int_0^{t+\delta t} \Xi_1(t,\tau)\Psi(u,\tau)\mathrm{d}\tau \right\| \\ &+ \left|\frac{\mu}{\eta\delta t}\right| \left\| \int_0^{\delta t} \Xi_2(\tau)\Psi(u,\tau)\mathrm{d}\tau \right\|.\end{aligned}$$

Applying Cauchy-Schwarz inequality, and using conditions (i)–(iii), we obtain

$$\|V\Psi\| \leq \beta\|\Psi\|, \quad \beta = \frac{|\eta|T + |\mu|[(D_1A + D_3)T + (D_1A + D_2A + D_3 + D_4)\delta t]}{|\eta|\delta t} < 1,$$

such that

$$|\mu| < \frac{|\eta|(\delta t - T)}{(D_1A + D_3)T + (D_1A + D_2A + D_3 + D_4)\delta t}, \quad 0 < \delta t < 1.$$

As a result, the integral operator V is normal, which leads immediately to the normality of the operator $\overline{V}$ when the condition (iv) is applied.

Secondly, for the continuity, we have

$$\|\overline{V}\Psi_1 - \overline{V}\Psi_2\| \leq \beta\|\Psi_1 - \Psi_2\|, \quad \beta < 1,$$

with

$$|\mu| < \frac{|\eta|(\delta t - T)}{(D_1A + D_3)T + (D_1A + D_2A + D_3 + D_4)\delta t}, \quad 0 < \delta t < 1.$$

Hence, $\overline{V}$ is a contraction operator, and by the Banach fixed point theorem, $\overline{V}$ has a unique fixed point, which is, of course, the only solution to IE (1.6). □

3. The system of Fredholm integral equations (SFIEs) of the second kind

The system of Fredholm integral equations (SFIEs) of the second kind plays a crucial role in mathematical modeling, particularly in solving inverse problems, boundary value problems, and integral equations. The versatility of SFIEs makes them invaluable in numerous scientific disciplines. They are extensively used in electromagnetic field simulations, inverse scattering problems, signal processing, and image reconstruction. By studying SFIEs, students can explore how these equations are applied to real-world problems and contribute to cutting-edge research developments.

3.1. Quadratic numerical method

The importance of quadratic numerical techniques derives from their numerous uses in mathematical physics problems, where the integral equations' eigenvalues and eigenfunctions are frequently examined and discussed. Additionally, this approach has several applications in the

real-world sciences, particularly in the areas of contact problems, mixed mechanics problems, and elasticity theory.

In this part, we express the V-FIE (1.6) of the second type as a system of second-kind Fredholm integral equations using the numerical technique. To do this, we split the time interval, $[0,T],\ 0 \le t \le T < 1$ as $0 = t_0 < t_1 < \cdots < t_m < \cdots < t_M = T$ where $t = t_m,\ m = 0,1,2,3,\ldots,M$; to get

$$\begin{aligned}\Psi(u,t_m) = Y(u,t_m) &- \frac{1}{\delta t}\int_0^{t_m}\Psi(u,\tau)\mathrm{d}\tau + \frac{\mu}{\eta\delta t}\int_0^{t_m+\delta t}\int_0^1 \Delta_1(t_m,\tau)k(u,v)\Psi(v,\tau)\mathrm{d}v\mathrm{d}\tau \\ &+ \frac{\mu}{\eta\delta t}\int_0^{\delta t}\int_0^1 \Delta_2(\tau)k(u,v)\Psi(v,\tau)\mathrm{d}v\mathrm{d}\tau \\ &+ \frac{\mu}{\eta\delta t}\int_0^{t_m+\delta t}\Xi_1(t_m,\tau)\Psi(u,\tau)\mathrm{d}\tau + \frac{\mu}{\eta\delta t}\int_0^{\delta t}\Xi_2(\tau)\Psi(u,\tau)\mathrm{d}\tau.\end{aligned} \tag{3.1}$$

Using the quadrature formula, we can calculate the following Volterra integral terms: In this work, the Volterra and Fredholm integrals are approximated using a composite quadrature rule based on a uniform partition of the integration intervals, where the weights λ_i, ν_{1i}, and ν_{2j} are computed accordingly.

$$\begin{aligned}&\int_0^{t_m+\delta t}\int_0^1 \Delta_1(t_m,\tau)k(u,v)\Psi(v,\tau)\mathrm{d}v\mathrm{d}\tau \approx \sum_{i=0}^{m}\nu_{1i}\int_0^1 \Delta_1(t_m,t_i)k(u,v)\Psi(v,t_i)\mathrm{d}v, \\ &\int_0^{t_m+\delta t}\Xi_1(t_m,\tau)\Psi(u,\tau)\mathrm{d}\tau \approx \sum_{i=0}^{m}\nu_{1i}\Xi_1(t_m,t_i)\Psi(u,t_i), \\ &\int_0^{t_m}\Psi(u,\tau)\mathrm{d}\tau \approx \sum_{i=0}^{m}\lambda_i\Psi(u,t_i).\end{aligned} \tag{3.2}$$

Equation (3.2) in equation (3.1) is used to obtain

$$\begin{aligned}\Psi(u,t_m) = Y(u,t_m) &- \frac{1}{\delta t}\sum_{i=0}^{m}\lambda_i\Psi(u,t_i) + \frac{\mu}{\eta\delta t}\sum_{i=0}^{m}\nu_{1i}\int_0^1 \Delta_1(t_m,t_i)k(u,v)\Psi(v,t_i)\mathrm{d}v \\ &+ \frac{\mu}{\eta\delta t}\int_0^{\delta t}\int_0^1 \Delta_2(\tau)k(u,v)\Psi(v,\tau)\mathrm{d}v\mathrm{d}\tau \\ &+ \frac{\mu}{\eta\delta t}\sum_{i=0}^{m}\nu_{1i}\Xi_1(t_m,t_i)\Psi(u,t_i) + \frac{\mu}{\eta\delta t}\int_0^{\delta t}\Xi_2(\tau)\Psi(u,\tau)\mathrm{d}\tau.\end{aligned} \tag{3.3}$$

Also, we divide the interval $[0,\delta t]$ into n subintervals of equal width, $0 = \tau_0 < \tau_1 < \tau_j < \ldots < \tau_n = \delta t$ where $(\tau_j - \tau_{j-1}) = \frac{1}{n}$ for $j = 1,2,\ldots,n$, and $n \le m$.

The Fredholm integral terms are calculated as follows:

$$\begin{aligned}&\int_0^{\delta t}\int_0^1 \Delta_2(\tau)k(u,v)\Psi(v,\tau)\mathrm{d}v\mathrm{d}\tau \approx \sum_{j=0}^{n}\nu_{2j}\int_0^1 \Delta_2(\tau_j)k(u,v)\Psi(v,\tau_j)\mathrm{d}v, \\ &\int_0^{\delta t}\Xi_2(\tau)\Psi(u,\tau)\mathrm{d}\tau \approx \sum_{j=0}^{n}\nu_{2j}\Xi_2(\tau_j)\Psi(u,\tau_j).\end{aligned} \tag{3.4}$$

Using equation (3.4) in the equation (3.3), we get

$$\begin{aligned}\Psi(u,t_m) =& Y(u,t_m) - \frac{1}{\delta t}\sum_{i=0}^{m}\lambda_i\Psi(u,t_i) + \frac{\mu}{\eta\delta t}\sum_{i=0}^{m}\nu_{1i}\int_0^1 \Delta_1(t_m,t_i)k(u,v)\Psi(v,t_i)\mathrm{d}v \\ &+ \frac{\mu}{\eta\delta t}\sum_{j=0}^{n}\nu_{2j}\int_0^1 \Delta_2(\tau_j)k(u,v)\Psi(v,\tau_j)\mathrm{d}v \\ &+ \frac{\mu}{\eta\delta t}\sum_{i=0}^{m}\nu_{1i}\Xi_1(t_m,t_i)\Psi(u,t_i) + \frac{\mu}{\eta\delta t}\sum_{j=0}^{n}\nu_{2j}\Xi_2(\tau_j)\Psi(u,\tau_j).\end{aligned} \tag{3.5}$$

Utilizing the notations shown below:

$$\Psi(u,t_m) = \Psi_m(u),\ Y(u,t_m) = Y_m(u),\ \Delta_1(t_m,t_i) = \Delta_{1,m,i},\ \Delta_2(\tau_j) = \Delta_{2,j}.$$

Equation (3.5) is transformed into

$$\begin{aligned}\Psi_m(u) =& Y_m(u) - \frac{1}{\delta t}\sum_{i=0}^{m}\lambda_i\Psi_i(u) + \frac{\mu}{\eta\delta t}\sum_{i=0}^{m}\nu_{1,i}\int_0^1 \Delta_{1,m,i}k(u,v)\Psi_i(v)\mathrm{d}v \\ &+ \frac{\mu}{\eta\delta t}\sum_{j=0}^{n}\nu_{2,j}\int_0^1 \Delta_{2,j}k(u,v)\Psi_j(v)\mathrm{d}v \\ &+ \frac{\mu}{\eta\delta t}\sum_{i=0}^{m}\nu_{1,i}\Xi_{1,m,i}\Psi_i(u) + \frac{\mu}{\eta\delta t}\sum_{j=0}^{n}\nu_{2,j}\Xi_{2,j}\Psi_j(u).\end{aligned} \tag{3.6}$$

According to equation (3.6), there are only a finite number of unknown functions $\Psi_m(u)$, $m = 0,1,\ldots,M$. Various techniques can be used to determine the solution of the system (3.6), for example, using Galerkin method, Picard's method, Expansion method, Collocation method, Quadrature method, etc. [6,25,27,28] to solve the system (3.6).

In the next section, we obtain the solution of the system (3.6), by using the shifted Legendre polynomials (SLPs) and least squares method (LSM), see [34,35].

3.2. Convergence analysis

To investigate the convergence of system (3.6), we assume the following conditions:

$$\max_i|\lambda_i| \le \alpha, \quad \max_j|\nu_{2,j}| \le \alpha_1, \quad \text{and} \quad \max_i|\nu_{1,i}| \le \alpha + \alpha_1. \tag{3.7}$$

Theorem 3.1. *If the series* $\sum_{m=0}^{\infty}\{\Phi_{m,n}(u)\}$, $\Phi_{m,n}(u) = \Psi_{m,n}(u) - \Psi_{m,n-1}(u)$ *is uniformly convergent, then* $\Psi_m(u)$ *represents the solution of system (3.6).*

Proof. We construct the sequence $\Psi_{m,n}(u)$ as follows

$$\begin{aligned}\Psi_{m,n}(u) =& Y_m(u) - \frac{1}{\delta t}\sum_{i=0}^{m}\lambda_i\Psi_{i,n-1}(u) + \frac{\mu}{\eta\delta t}\sum_{i=0}^{m}\nu_{1,i}\int_0^1 \Delta_{1,m,i}k(u,v)\Psi_{i,n-1}(v)\mathrm{d}v \\ &+ \frac{\mu}{\eta\delta t}\sum_{j=0}^{n}\nu_{2,j}\int_0^1 \Delta_{2,j}k(u,v)\Psi_{j,n-1}(v)\mathrm{d}v \\ &+ \frac{\mu}{\eta\delta t}\sum_{i=0}^{m}\nu_{1,i}\Xi_{1,m,i}\Psi_{i,n-1}(u) + \frac{\mu}{\eta\delta t}\sum_{j=0}^{n}\nu_{2,j}\Xi_{2,j}\Psi_{j,n-1}(u).\end{aligned} \tag{3.8}$$

Create the function $\Phi_{m,n}(u)$ such that $\Phi_{m,n}(u) = \Psi_{m,n}(u) - \Psi_{m,n-1}(u)$. According to that, the integral Eq. (3.8), becomes

$$\begin{aligned}\Phi_{m,n}(u) = \frac{-1}{\delta t}\sum_{i=0}^{m}\lambda_i(\Psi_{i,n-1}(u) - \Psi_{i,n-2}(u)) \\ + \left|\frac{\mu}{\eta\delta t}\right|\sum_{i=0}^{m}\nu_{1,i}\int_0^1 \Delta_{1,m,i}k(u,v)(\Psi_{i,n-1}(v) - \Psi_{i,n-2}(v))\mathrm{d}v \\ + \left|\frac{\mu}{\eta\delta t}\right|\sum_{j=0}^{n}\nu_{2,j}\int_0^1 \Delta_{2,j}k(u,v)(\Psi_{j,n-1}(v) - \Psi_{j,n-2}(v))\mathrm{d}v \\ + \left|\frac{\mu}{\eta\delta t}\right|\sum_{i=0}^{m}\nu_{1,i}\Xi_{1,m,i}(\Psi_{i,n-1}(u) - \Psi_{i,n-2}(u)) \\ + \left|\frac{\mu}{\eta\delta t}\right|\sum_{j=0}^{n}\nu_{2,j}\Xi_{2,j}(\Psi_{j,n-1}(u) - \Psi_{j,n-2}(u)).\end{aligned}$$

By applying the norm properties and conditions (i)–(iii), (3.7), we obtain

$$\begin{aligned}\|\Phi_{m,n}(u)\| \le \left|\frac{-1}{\delta t}\right|\alpha\sum_{i=0}^{m}\|\Psi_{i,n-1}(u) - \Psi_{i,n-2}(u)\| \\ + \left|\frac{\mu}{\eta\delta t}\right|(\alpha+\alpha_1)D_1A\sum_{i=0}^{m}\|\Psi_{i,n-1}(u) - \Psi_{i,n-2}(u)\| \\ + \left|\frac{\mu}{\eta\delta t}\right|\alpha_1 D_2A\sum_{j=0}^{n}\|\Psi_{j,n-1}(u) - \Psi_{j,n-2}(u)\| \\ + \left|\frac{\mu}{\eta\delta t}\right|(\alpha+\alpha_1)D_3\sum_{i=0}^{m}\|\Psi_{i,n-1}(u) - \Psi_{i,n-2}(u)\| \\ + \left|\frac{\mu}{\eta\delta t}\right|\alpha_1 D_4\sum_{j=0}^{n}\|\Psi_{j,n-1}(u) - \Psi_{j,n-2}(u)\|,\end{aligned}$$

hence, we have

$$\|\Phi_{m,n}(u)\| \le \frac{|\eta|\alpha + |\mu|[(D_1A+D_3)\alpha + (D_1A+D_2A+D_3+D_4)\alpha_1]}{|\eta|\delta t}\sum_{i=0}^{m}\|(\Phi_{i,n-1}(u)\|,$$

for $n = 1$ and using condition (iv), we obtain

$$\|\Phi_{m,1}(u)\| \;\le\; \frac{|\eta|\alpha + |\mu|[(D_1A+D_3)\alpha + (D_1A+D_2A+D_3+D_4)\alpha_1]}{|\eta|\delta t}\; m\; A_1,$$

and by induction, we get

$$\|\Phi_{m,n}(u)\| \le (\beta_m)^n\; A_1, \quad \beta_m = \frac{|\eta|\alpha + |\mu|[(D_1A+D_3)\alpha + (D_1A+D_2A+D_3+D_4)\alpha_1]}{|\eta|\delta t}m < 1. \tag{3.9}$$

Inequality (3.9) indicates that the system (3.6) is uniformly convergent and has a unique solution as $n \to \infty$. □

4. The properties of Legendre polynomials

This part starts with a review of some basic facts about Legendre polynomials. Then, we introduce the main features of the SLPs and derive some of the fundamental mathematical tools needed to create the proposed method. Legendre polynomials are orthogonal functions that are utilised as fundamental approximations. Compared to other orthogonal polynomials (Chebyshev polynomials, etc.), they display a convenient and easy-to-calculate form. Legendre polynomials have an interval from -1 to 1.

4.1. Legendre polynomials and shifted Legendre polynomials

The following recurrence formula, which defines the Legendre polynomials on the interval $[-1, 1]$, can be used to get the well-known orthogonal polynomials of degree ℓ in v. For further information, see [17]:

$$P_{\ell+1}(v) = \frac{(2\ell+1)}{(\ell+1)} v P_\ell(v) - \frac{\ell}{(\ell+1)} P_{\ell-1}(v), \quad \ell = 1, 2, \ldots, \tag{4.1}$$

with

$$P_0(v) = 1, \quad P_1(v) = v.$$

The weighted space $L^2_{w(v)}[-1, 1] \equiv L^2[-1, 1]$ can be defined since the Legendre weight function $w(v) = 1$ is normal, provided with the inner product and the standard of the following:

$$\langle f(v), g(v) \rangle = \int_{-1}^{1} f(v) g(v) \mathrm{d}v, \quad \|f(v)\| = \langle f(v), f(v) \rangle^{1/2}.$$

Therefore, a complete $L^2[-1, 1]$-orthogonal system is formed by the set of Legendre polynomials, and

$$\langle P_{\ell_1}(v), P_{\ell_2}(v) \rangle = \frac{2}{(2\ell_1+1)} \delta_{\ell_1 \ell_2},$$

where $\delta_{\ell_1 \ell_2}$ is the Kronecker function. By applying the change of variable $v = 2u - 1$, we provide the SLPs using these polynomials on the interval $u \in [0, 1]$. The SLPs $P_\ell(2u-1)$, which are represented by $L_\ell(u)$, are all we have yet to study. Next, the following recurrence relation can be used to construct the SLPs of degree ℓ:

$$L_{\ell+1}(u) = \frac{(2\ell+1)(2u-1)}{(\ell+1)} L_\ell(u) - \frac{\ell}{(\ell+1)} L_{\ell-1}(u), \quad \ell = 1, 2, \ldots, \tag{4.2}$$

when $u \in [0, 1]$ and the following are the fundamental properties of the SLPs:

$$\begin{aligned}
&L_0(u) = 1,\\
&L_1(u) = 2u - 1,\\
&L_2(u) = 6u^2 - 6u + 1,\\
&L_3(u) = 20u^3 - 30u^2 + 12u - 1,\\
&\quad \vdots\\
&1 = L_0(u),\\
&u = (1/2)[L_0(u) + L_1(u)],
\end{aligned}$$

$$u^2 = (1/6)[2L_0(u) + 3L_1(u) + L_2(u)],$$
$$u^3 = (1/20)[5L_0(u) + 9L_1(u) + 5L_2(u) + L_3(u)],$$

and

$$L_\ell(u) = (-1)^\ell L_\ell(1-u).$$

It is possible to write the binomial expansion of the SLPs as

$$\begin{aligned} L_\ell(u) &= \sum_{i=0}^{\ell} (-1)^{\ell+i} \frac{(\ell+i)!u^i}{(\ell-1)!(i!)^2}, \quad \ell \in \mathbb{N} \\ &= \sum_{i=0}^{\ell} (-1)^i \frac{(2\ell-i)!u^{\ell-i}}{[(\ell-1)!]^2 i!} \\ &= \frac{1}{\ell!}\frac{\mathrm{d}^\ell}{\mathrm{d}u^\ell}\left[u^\ell(u-1)^\ell\right]. \end{aligned} \tag{4.3}$$

Recall that

$$L_\ell(0) = (-1)^\ell, \quad L_\ell(1) = 1.$$

Regarding the weight function $w_s(u) = 1$ on the interval $[0, 1]$ corresponding to the inner product given below, these polynomials satisfy the following orthogonality condition:

$$\langle L_{\ell_1}(u), L_{\ell_2}(u)\rangle = \int_0^1 L_{\ell_1}(u)L_{\ell_2}(u)w_s(u)\mathrm{d}u = \frac{1}{(2\ell_1+1)}\delta_{\ell_1\ell_2}.$$

4.2. Shifted Legendre expansion and truncated approximation

The function $\Psi(u) \in L^2_{w_s(u)}[0, 1]$ can be expanded concerning the SLPs as follows, as known:

$$\Psi(u) = \sum_{\ell=0}^{\infty} \beta_\ell L_\ell(u), \tag{4.4}$$

where the coefficients of the series are denoted by β_ℓ. Therefore, given a polynomial of degree N, $\Psi(u)$ can be represented as follows in terms of the SLPs:

$$\Psi_N(u) = \sum_{\ell=0}^{N} \beta_\ell L_\ell(u) = \mathbf{B}^T\psi(u), \tag{4.5}$$

where the vector $\mathbf{B} = [\beta_0, \beta_1, \ldots, \beta_N]^T$ and its component values are based on the integration that follows:

$$\beta_\ell = (2\ell+1)\int_0^1 \Psi_N(u)L_\ell(u)w_s(u)\mathrm{d}u, \quad \ell = 0, 1, 2, \ldots, N. \tag{4.6}$$

Assume that $\psi(u)$, the shifted Legendre vector, is expressed as

$$\psi(u) = [L_0(u), L_1(u), \ldots, L_N(u)]^T, \tag{4.7}$$

as well as presume

$$T_N(u) = [1, u, u^2, \ldots, u^N]^T, \tag{4.8}$$

then the following is an expression for the vector $\psi(u)$

$$\psi(u) = AT_N(u), \tag{4.9}$$

where A is $(N+1)\times(N+1)$ square matrix provided by

$$(a_{m,n})_{0\le m,n\le N} = \begin{cases} 0, & m < n, \\ (-1)^{N-m}\dfrac{\Gamma(N+1)\Gamma(N+m+1)}{\Gamma(N+1)\Gamma(N-m+1)(\Gamma(m+1))^2}, & m \ge n. \end{cases} \tag{4.10}$$

The diagonal elements of matrix A, which is a $N+1$ order lower triangular matrix, are all positive integers. The linear transformation can be used to convert matrix A into the $N+1$ order identity matrix. Thus, A is an invertible matrix. As an example, if $N=4$, the square matrix A can be found by

$$\begin{pmatrix} 1 & 0 & 0 & 0 & 0 \\ -1 & 2 & 0 & 0 & 0 \\ 1 & -6 & 6 & 0 & 0 \\ -1 & 12 & -30 & 20 & 0 \\ 1 & -20 & 90 & -140 & 70 \end{pmatrix}.$$

Thus, utilizing equation (4.8), we conclude

$$T_N(u) = A^{-1}\psi(u). \tag{4.11}$$

5. Solution of the system of Fredholm integral equations of the second kind (3.6)

This section explains the method of using SLPs to solve the main problem numerically using the LSM. As a result, the problem will be transformed into an algebraic system of equations with collocation points where numerical solutions can be found. The following is an expression for a function $\Psi_m(u)$ in terms of SLPs:

$$\Psi_m(u) = \sum_{\ell=0}^{\infty} \beta_{\ell,m} L_\ell(u). \tag{5.1}$$

In actuality, we take into account the SLPs about u of the $(N+1)$-terms so that

$$\Psi_{m,N}(u) = \sum_{\ell=0}^{N} \beta_{\ell,m} L_\ell(u), \tag{5.2}$$

where,

$$\beta_{\ell,m} = (2\ell+1)\int_0^1 \Psi_{m,N}(u)L_\ell(u)\mathrm{d}u, \quad \ell = 0,1,2,\ldots,N. \tag{5.3}$$

We obtain the following equation from the system (3.6) to simplify the presented method technique:

$$\begin{aligned}\Lambda_m\Psi_m(u) =& Y_m(u) - \frac{1}{\delta t}\sum_{i=0}^{m-1}\lambda_i\Psi_i(u) + \frac{\mu}{\eta\delta t}\sum_{i=0}^{m}\nu_{1,i}\int_0^1 \Delta_{1,m,i}k(u,v)\Psi_i(v)\mathrm{d}v \\ &+ \frac{\mu}{\eta\delta t}\sum_{j=0}^{n}\nu_{2,j}\int_0^1 \Delta_{2,j}k(u,v)\Psi_j(v)\mathrm{d}v \\ &+ \frac{\mu}{\eta\delta t}\sum_{i=0}^{m-1}\nu_{1,i}\Xi_{1,m,i}\Psi_i(u) + \frac{\mu}{\eta\delta t}\sum_{j=0}^{n}\nu_{2,j}\Xi_{2,j}\Psi_j(u), \end{aligned} \tag{5.4}$$

where, $\Lambda_m = \frac{\lambda_m}{\delta t} - \frac{\mu}{\eta\delta t}\nu_{1,m}\Xi_{1,m,m}$.

Putting (5.2) to use in (5.4), in this way:

$$\begin{aligned}\Lambda_m\sum_{\ell=0}^{N}\beta_{\ell,m}L_\ell(u) =& Y_m(u) - \frac{1}{\delta t}\sum_{i=0}^{m-1}\sum_{\ell=0}^{N}\lambda_i\beta_{\ell,i}L_\ell(u) \\ &+ \frac{\mu}{\eta\delta t}\sum_{i=0}^{m}\nu_{1,i}\int_0^1 \Delta_{1,m,i}k(u,v)\left[\sum_{\ell=0}^{N}\beta_{\ell,i}L_\ell(v)\right]\mathrm{d}v \\ &+ \frac{\mu}{\eta\delta t}\sum_{j=0}^{n}\nu_{2,j}\int_0^1 \Delta_{2,j}k(u,v)\left[\sum_{\ell=0}^{N}\beta_{\ell,j}L_\ell(v)\right]\mathrm{d}v \\ &+ \frac{\mu}{\eta\delta t}\sum_{i=0}^{m-1}\sum_{\ell=0}^{N}\nu_{1,i}\Xi_{1,m,i}\beta_{\ell,i}L_\ell(u) + \frac{\mu}{\eta\delta t}\sum_{j=0}^{n}\sum_{\ell=0}^{N}\nu_{2,j}\Xi_{2,j}\beta_{\ell,j}L_\ell(u). \end{aligned} \tag{5.5}$$

For any $u \in [0,1]$, $E_{m,N}(u) = \Psi_{m,N}(u) - \Psi_m(u)$ is called the N-order remaining elements of Eq. (5.4), where

$$\begin{aligned}E_{m,N}(u) =& \frac{1}{\delta t}\sum_{i=0}^{m-1}\lambda_i(\Psi_i(u) - \Psi_{i,N}(u)) + \frac{\mu}{\eta\delta t}\sum_{i=0}^{m}\nu_{1,i}\int_0^1 \Delta_{1,m,i}k(u,v)(\Psi_{i,N}(v) - \Psi_i(v))\mathrm{d}v \\ &+ \frac{\mu}{\eta\delta t}\sum_{j=0}^{n}\nu_{2,j}\int_0^1 \Delta_{2,j}k(u,v)(\Psi_{j,N}(v) - \Psi_j(v))\mathrm{d}v \\ &+ \frac{\mu}{\eta\delta t}\sum_{i=0}^{m-1}\nu_{1,i}\Xi_{1,m,i}(\Psi_{i,N}(u) - \Psi_i(u)) + \frac{\mu}{\eta\delta t}\sum_{j=0}^{n}\nu_{2,j}\Xi_{2,j}(\Psi_{j,N}(u) - \Psi_j(u)). \end{aligned}$$

Remark 5.1. If $E_{m,N}(u) = 0$, then $\Psi_m(u) = \Psi_{m,N}(u)$; if $\lim_{N\to\infty} E_{m,N}(u) = 0$, then $\lim_{N\to\infty}\Psi_{m,N}(u) = \Psi_m(u)$.

Remark 5.2. For any $u \in [0,1]$, if $E_{m,N}(u) \equiv 0$, then $\Psi_m(u)$ is an exact solution of Eq. (5.4); if $\lim_{N\to\infty} E_{m,N}(u) = 0$, then $\Psi_{m,N}(u)$ converges to the exact solution of Eq. (5.4).

From equation (5.5), we can obtain the following expression:

$$\begin{aligned}R_m(u,\beta_{0,m},\beta_{1,m},\ldots,\beta_{N,m}) =& \Lambda_m\sum_{\ell=0}^{N}\beta_{\ell,m}L_\ell(u) - Y_m(u) + \frac{1}{\delta t}\sum_{i=0}^{m-1}\sum_{\ell=0}^{N}\lambda_i\beta_{\ell,i}L_\ell(u) \\ &- \frac{\mu}{\eta\delta t}\sum_{i=0}^{m}\nu_{1,i}\int_0^1 \Delta_{1,m,i}k(u,v)\left[\sum_{\ell=0}^{N}\beta_{\ell,i}L_\ell(v)\right]\mathrm{d}v \end{aligned}$$

$$- \frac{\mu}{\eta\delta t}\sum_{j=0}^{n}\nu_{2,j}\int_0^1 \Delta_{2,j}k(u,v)\left[\sum_{\ell=0}^{N}\beta_{\ell,j}L_\ell(v)\right]\mathrm{d}v$$
$$- \frac{\mu}{\eta\delta t}\sum_{i=0}^{m-1}\sum_{\ell=0}^{N}\nu_{1,i}\Xi_{1,m,i}\beta_{\ell,i}L_\ell(u) - \frac{\mu}{\eta\delta t}\sum_{j=0}^{n}\sum_{\ell=0}^{N}\nu_{2,j}\Xi_{2,j}\beta_{\ell,j}L_\ell(u),$$

where, R_m denotes the residual function associated with the m-th time level.

Let

$$S_m(\beta_{0,m},\beta_{1,m},\ldots,\beta_{N,m}) = \int_0^1 \left[R_m(z,\beta_{0,m},\beta_{1,m},\ldots,\beta_{N,m})\right]^2 w(z)\mathrm{d}z.$$

You can define any positive function on the interval $[0,1]$ as $w(z)$. Usually, it's referred to as the weight function. For simplicity, we assume $w(z)=1$ in this work.

Therefore

$$\begin{aligned}S_m(\beta_{0,m},\beta_{1,m},\ldots,\beta_{N,m}) = \int_0^1 \Bigg[&\Lambda_m\sum_{\ell=0}^{N}\beta_{\ell,m}L_\ell(z) - Y_m(z) + \frac{1}{\delta t}\sum_{i=0}^{m-1}\sum_{\ell=0}^{N}\lambda_i\beta_{\ell,i}L_\ell(z)\\ &- \frac{\mu}{\eta\delta t}\sum_{i=0}^{m}\nu_{1,i}\int_0^1 \Delta_{1,m,i}k(z,v)\left(\sum_{\ell=0}^{N}\beta_{\ell,i}L_\ell(v)\right)\mathrm{d}v\\ &- \frac{\mu}{\eta\delta t}\sum_{j=0}^{n}\nu_{2,j}\int_0^1 \Delta_{2,j}k(z,v)\left(\sum_{\ell=0}^{N}\beta_{\ell,j}L_\ell(v)\right)\mathrm{d}v\\ &- \frac{\mu}{\eta\delta t}\sum_{i=0}^{m-1}\sum_{\ell=0}^{N}\nu_{1,i}\Xi_{1,m,i}\beta_{\ell,i}L_\ell(z) - \frac{\mu}{\eta\delta t}\sum_{j=0}^{n}\sum_{\ell=0}^{N}\nu_{2,j}\Xi_{2,j}\beta_{\ell,j}L_\ell(z)\Bigg]^2\mathrm{d}z.\end{aligned} \tag{5.6}$$

The unknown coefficients $\beta_{\ell,m};\ \ell=0,1,\ldots,N$ are obtained by minimizing the least-squares functional $S_m(\beta_{0,m},\beta_{1,m},\ldots,\beta_{N,m})$.

To determine the minimum value of S_m, we set

$$\frac{\partial S_m}{\partial \beta_{\ell,m}} = 0, \quad \ell = 0,1,\ldots,N. \tag{5.7}$$

Hence, we have

$$\begin{aligned}\int_0^1 \Bigg[&\Lambda_m\sum_{\ell=0}^{N}\beta_{\ell,m}L_\ell(z) - Y_m(z) + \frac{1}{\delta t}\sum_{i=0}^{m-1}\sum_{\ell=0}^{N}\lambda_i\beta_{\ell,i}L_\ell(z)\\ &- \frac{\mu}{\eta\delta t}\sum_{i=0}^{m}\nu_{1,i}\int_0^1 \Delta_{1,m,i}k(z,v)\left(\sum_{\ell=0}^{N}\beta_{\ell,i}L_\ell(v)\right)\mathrm{d}v\\ &- \frac{\mu}{\eta\delta t}\sum_{j=0}^{n}\nu_{2,j}\int_0^1 \Delta_{2,j}k(z,v)\left(\sum_{\ell=0}^{N}\beta_{\ell,j}L_\ell(v)\right)\mathrm{d}v\\ &- \frac{\mu}{\eta\delta t}\sum_{i=0}^{m-1}\sum_{\ell=0}^{N}\nu_{1,i}\Xi_{1,m,i}\beta_{\ell,i}L_\ell(z) - \frac{\mu}{\eta\delta t}\sum_{j=0}^{n}\sum_{\ell=0}^{N}\nu_{2,j}\Xi_{2,j}\beta_{\ell,j}L_\ell(z)\Bigg]\end{aligned}$$

$$\times \{\Lambda_m L_\wp(z) + \frac{1}{\delta t}\sum_{i=0}^{m-1}\lambda_i L_\wp(z) - \frac{\mu}{\eta\delta t}\sum_{i=0}^{m}\nu_{1,i}\int_0^1 \Delta_{1,m,i}k(z,v)L_\wp(v)\mathrm{d}v$$
$$- \frac{\mu}{\eta\delta t}\sum_{j=0}^{n}\nu_{2,j}\int_0^1 \Delta_{2,j}k(z,v)L_\wp(v)\mathrm{d}v$$
$$- \frac{\mu}{\eta\delta t}\sum_{i=0}^{m-1}\nu_{1,i}\Xi_{1,m,i}L_\wp(z) - \frac{\mu}{\eta\delta t}\sum_{j=0}^{n}\nu_{2,j}\Xi_{2,j}L_\wp(z)\Bigg\}\mathrm{d}z = 0. \tag{5.8}$$

We can get a system of $(N+1)$ linear equations with $(N+1)$ unknown coefficients $\beta_{\wp,m}$'s by evaluating the previous equation for $\wp = 0, 1, \ldots, N$. Matrices form can be used to build this system in the following way:

$$H = \begin{pmatrix} \int_0^1 R_m(z,\beta_{0,m})\Im_0\mathrm{d}z & \int_0^1 R_m(z,\beta_{1,m})\Im_0\mathrm{d}z & \cdots & \int_0^1 R_m(z,\beta_{N,m})\Im_0\mathrm{d}z \\ \int_0^1 R_m(z,\beta_{0,m})\Im_1\mathrm{d}z & \int_0^1 R_m(z,\beta_{1,m})\Im_1\mathrm{d}z & \cdots & \int_0^1 R_m(z,\beta_{N,m})\Im_1\mathrm{d}z \\ \vdots & \vdots & \vdots & \vdots \\ \int_0^1 R_m(z,\beta_{0,m})\Im_N\mathrm{d}z & \int_0^1 R_m(z,\beta_{1,m})\Im_N\mathrm{d}z & \cdots & \int_0^1 R_m(z,\beta_{N,m})\Im_N\mathrm{d}z \end{pmatrix}, \tag{5.9}$$

and

$$Q = \begin{pmatrix} \int_0^1 Y_m(z)\Im_0\mathrm{d}z \\ \int_0^1 Y_m(z)\Im_1\mathrm{d}z \\ \vdots \\ \int_0^1 Y_m(z)\Im_N\mathrm{d}z \end{pmatrix}, \tag{5.10}$$

where

$$R_m(z,\beta_{\ell,m}) = \Lambda_m\sum_{\ell=0}^{N}\beta_{\ell,m}L_\ell(z) + \frac{1}{\delta t}\sum_{i=0}^{m-1}\sum_{\ell=0}^{N}\lambda_i\beta_{\ell,i}L_\ell(z)$$
$$- \frac{\mu}{\eta\delta t}\sum_{i=0}^{m}\nu_{1,i}\int_0^1 \Delta_{1,m,i}k(z,v)\left(\sum_{\ell=0}^{N}\beta_{\ell,i}L_\ell(v)\right)\mathrm{d}v$$
$$- \frac{\mu}{\eta\delta t}\sum_{j=0}^{n}\nu_{2,j}\int_0^1 \Delta_{2,j}k(z,v)\left(\sum_{\ell=0}^{N}\beta_{\ell,j}L_\ell(v)\right)\mathrm{d}v$$
$$- \frac{\mu}{\eta\delta t}\sum_{i=0}^{m-1}\sum_{\ell=0}^{N}\nu_{1,i}\Xi_{1,m,i}\beta_{\ell,i}L_\ell(z) - \frac{\mu}{\eta\delta t}\sum_{j=0}^{n}\sum_{\ell=0}^{N}\nu_{2,j}\Xi_{2,j}\beta_{\ell,j}L_\ell(z), \tag{5.11}$$

with

$$\Im_\wp = \Lambda_m L_\wp(z) + \frac{1}{\delta t}\sum_{i=0}^{m-1}\lambda_i L_\wp(z) - \frac{\mu}{\eta\delta t}\sum_{i=0}^{m}\nu_{1,i}\int_0^1 \Delta_{1,m,i}k(z,v)L_\wp(v)\mathrm{d}v$$

$$- \frac{\mu}{\eta\delta t}\sum_{j=0}^{n}\nu_{2,j}\int_0^1 \Delta_{2,j}k(z,v)L_{\wp}(v)\mathrm{d}v$$
$$- \frac{\mu}{\eta\delta t}\sum_{i=0}^{m-1}\nu_{1,i}\Xi_{1,m,i}L_{\wp}(z) - \frac{\mu}{\eta\delta t}\sum_{j=0}^{n}\nu_{2,j}\Xi_{2,j}L_{\wp}(z). \tag{5.12}$$

We can determine the values of the unknown coefficients and the approximate solution of (5.4) by solving the system described above.

Definition 5.1. For every $\varepsilon > 0$, if $\int_0^1 R_m^2(u,\beta_{0,m},\beta_{1,m},\ldots,\beta_{N,m})\mathrm{d}u \le \varepsilon$, then $\Psi_{m,N}(u)$ is called an ε-approximate solution of Eq. (5.4).

Remark 5.3. If $\lim_{N\to\infty}\int_0^1 R_m^2(u,\beta_{0,m},\beta_{1,m},\ldots,\beta_{N,m})\mathrm{d}u = 0$, then the approximation solution $\Psi_{m,N}(u) = \sum_{\ell=0}^{N}\beta_{\ell,m}L_\ell(u)$ converges to the exact solution $\Psi_m(u)$ of Eq. (5.4).

The resulting algebraic system at each time level m is a dense linear system of size$(N+1)\times(N+1)$ and is solved using a standard direct method such as LU decomposition. Consequently, the computational cost scales as $O((N+1)^3)$ per time level.

6. Convergence analysis

We provide a convergence study for the proposed method in this section. The approximation solution $\Psi_{m,N}(u)$ should converge to the exact solution $\Psi_m(u)$ of Eq. (5.4) as $N\to\infty$, according to the technique of solving in Section 5. The following theorem establishes the convergence of the LSM:

Theorem 6.1. *Let $\Psi_m(u)$ be the exact solution of Eq. (5.4), and assume that $\Psi_{m,N}(u)$ is the approximation solution provided on $[0,1]$. If $\exists\Theta_{m,N}(u) = \sum_{\ell=0}^{N}\alpha_{\ell,m}L_\ell(u)$, such that $\forall u\in[0,1]$, $\lim_{N\to\infty}\Theta_{m,N}(u) = \Psi_m(u)$, then*

$$\lim_{N\to\infty}\int_0^1 R_m^2(u,\beta_{0,m},\beta_{1,m},\ldots,\beta_{N,m})\mathrm{d}u = 0.$$

Proof. The following inequality is valid based on the way the coefficients of the approximation solution $\Psi_{m,N}(u)$ are calculated and taking into account the relations (5.1)–(5.6):

$$0 \le \int_0^1 R_m^2(u,\beta_{0,m},\beta_{1,m},\ldots,\beta_{N,m})\mathrm{d}u \le \int_0^1 R_m^2(u,\alpha_{0,m},\alpha_{1,m},\ldots,\alpha_{N,m})\mathrm{d}u.$$

Thus, it can be concluded that

$$0 \le \lim_{N\to\infty}\int_0^1 R_m^2(u,\beta_{0,m},\beta_{1,m},\ldots,\beta_{N,m})\mathrm{d}u \le \lim_{N\to\infty}\int_0^1 R_m^2(u,\alpha_{0,m},\alpha_{1,m},\ldots,\alpha_{N,m})\mathrm{d}u.$$

Since $\lim_{N\to\infty}\Theta_{m,N}(u) = \Psi_m(u)$, that is, $\int_0^1 R_m^2(u,\alpha_{0,m},\alpha_{1,m},\ldots,\alpha_{N,m})\mathrm{d}u = 0$. Thus,

$$\lim_{N\to\infty}\int_0^1 R_m^2(u,\beta_{0,m},\beta_{1,m},\ldots,\beta_{N,m})\mathrm{d}u = 0.$$

It is now complete to prove this theorem. □

7. Numerical problems

In this section, several numerical examples are presented to demonstrate the accuracy, convergence, and effectiveness of the proposed shifted Legendre least-squares method for solving phase-lagged Volterra–Fredholm integral equations. The selected examples cover different problem settings, including nonlinear and linear equations as well as kernels with specific structural properties, such as symmetry. Whenever possible, exact solutions are used to provide a direct and reliable assessment of the numerical accuracy.

The performance of the method is evaluated using the maximum absolute error, and the numerical results are reported for different time levels and truncation orders. The examples are designed to validate the theoretical analysis presented in the previous sections and to illustrate the practical efficiency and stability of the proposed approach.

Example 7.1. Consider the following V-FIE with a phase-lag $\delta t = 0.7$:

$$\begin{aligned}\Psi(u,t+0.7) &= y(u,t+0.7) + 0.01\int_0^{t+0.7}\int_0^1 ((t+0.7)^2\tau)(u^2v)\Psi(v,\tau)\mathrm{d}v\mathrm{d}\tau \\ &\quad + 0.01\int_0^{t+0.7}(t+0.7)\tau^2\Psi(u,\tau)\mathrm{d}\tau, \\ &\text{“}\Psi(u,0)=0; \quad y(u,t+0.7) = (t+0.7)u^2 - 0.00333333\ (t+0.7)^5u^2.\text{”}\end{aligned} \tag{7.1}$$

The proposed shifted Legendre least-squares method is applied to this problem for several time levels $t_m \in [0, 0.6]$ and truncation orders N.

Tables 1–3 report the absolute errors for $t_0 = 0$, $t_1 = 0.3$, and $t_2 = 0.6$, respectively. The numerical results show a clear and systematic decrease in the error as the truncation order N increases, confirming the convergence of the proposed approximation scheme.

Figures 1–3 illustrate the comparison between the exact solution and the numerical solutions at representative time levels. The approximate solutions closely match the exact solution over the entire spatial domain $u \in [0, 1]$, and the agreement improves noticeably as N increases. These results demonstrate that the proposed method provides accurate and stable numerical solutions for phase-lagged Volterra–Fredholm integral equations, even for relatively small truncation orders.

Table 1. Absolute errors for Example 7.1 at $t_0 = 0$ for different truncation orders N.

u_i	$N = 4$	$N = 5$	$N = 7$	$N = 9$
0	0	0	0	0
0.1	1.538E-07	1.355E-07	3.547E-08	1.570E-09
0.2	3.685E-07	2.158E-07	5.215E-08	2.525E-09
0.3	4.528E-07	2.587E-07	6.521E-08	3.690E-09
0.4	4.988E-07	3.102E-07	7.521E-08	5.247E-09
0.5	6.521E-07	4.326E-07	8.255E-08	7.458E-09
0.6	7.410E-07	4.521E-07	9.254E-08	6.325E-08
0.7	3.698E-06	5.299E-07	5.231E-07	7.215E-08
0.8	4.529E-06	6.255E-07	5.625E-07	8.574E-08
0.9	5.214E-06	2.587E-06	6.321E-07	9.585E-08
1	6.325E-06	3.015E-06	7.524E-07	4.127E-07

Table 2. Absolute errors for Example 7.1 at $t_1 = 0.3$ for different truncation orders N.

u_i	$N = 4$	$N = 5$	$N = 7$	$N = 9$
0	0	0	0	0
0.1	5.214E-07	3.658E-07	3.610E-08	1.201E-08
0.2	5.925E-07	4.366E-07	7.521E-08	3.658E-08
0.3	6.254E-07	5.237E-07	8.521E-08	5.874E-08
0.4	7.385E-07	6.255E-07	9.025E-08	6.985E-08
0.5	8.520E-07	6.529E-07	1.366E-07	8.549E-08
0.6	8.874E-07	7.125E-07	2.741E-07	1.712E-07
0.7	9.174E-06	7.521E-07	6.358E-07	2.587E-07
0.8	9.574E-06	8.521E-07	7.521E-07	4.751E-07
0.9	3.855E-05	5.874E-06	9.633E-07	5.180E-07
1	4.126E-05	7.542E-06	2.587E-06	6.527E-07

Table 3. Absolute errors for Example 7.1 at $t_2 = 0.6$ for different truncation orders N.

u_i	$N = 4$	$N = 5$	$N = 7$	$N = 9$
0	3.524E-06	2.547E-06	2.689E-07	4.739E-08
0.1	5.968E-06	4.752E-06	3.588E-07	5.213E-08
0.2	6.524E-06	5.412E-06	3.987E-07	7.125E-08
0.3	7.521E-06	6.854E-06	4.752E-07	7.963E-08
0.4	8.621E-06	7.582E-06	6.325E-07	8.524E-08
0.5	9.633E-06	3.658E-05	8.985E-07	9.325E-08
0.6	4.321E-05	4.588E-05	9.630E-07	3.652E-07
0.7	5.633E-05	5.269E-05	3.652E-06	2.857E-06
0.8	5.921E-05	5.585E-05	5.396E-06	3.625E-06
0.9	6.125E-05	5.874E-05	7.412E-06	5.874E-06
1	1.521E-04	6.547E-05	7.520E-05	6.925E-06

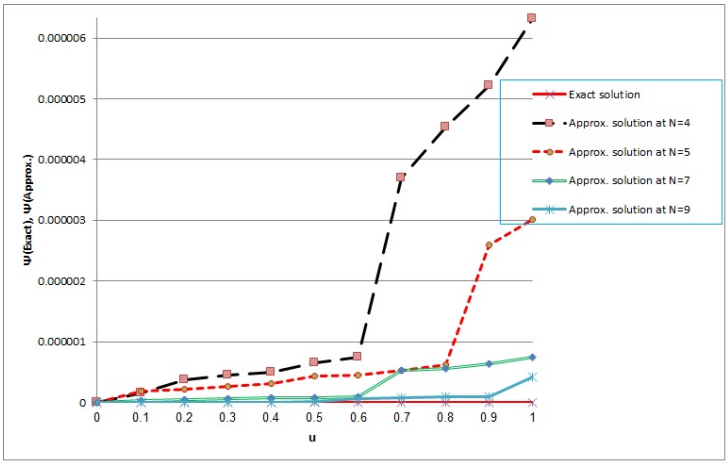

Figure 1. Exact and approximate solutions of $\Psi(u,t)$ at $(t_0 = 0)$ obtained using the shifted Legendre least-squares method for different truncation orders N.

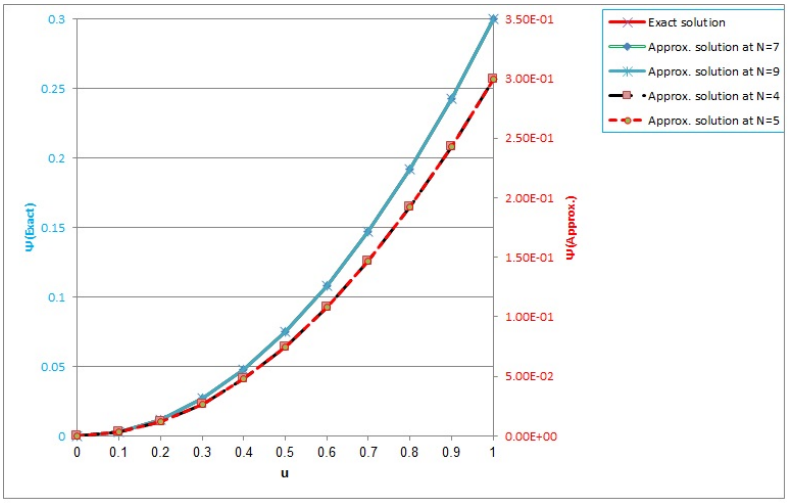

Figure 2. Exact and approximate solutions of $\Psi(u,t)$ at $(t_1 = 0.3)$ obtained using the shifted Legendre least-squares method for different truncation orders N.

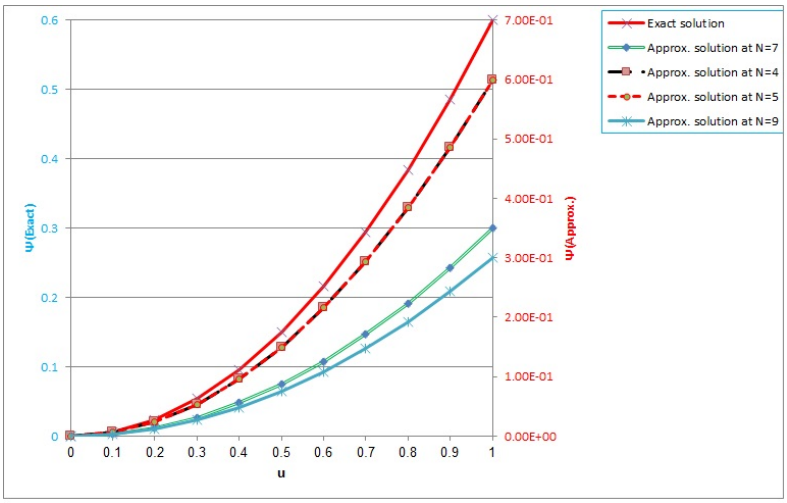

Figure 3. Exact and approximate solutions of $\Psi(u,t)$ at $(t_2 = 0.6)$ obtained using the shifted Legendre least-squares method for different truncation orders N.

Example 7.2. Consider the linear V-FIE [16, 37]

$$\Psi(t) = t - e^{t} + e^{-t} + 1 + \int_0^1 e^{(t+\tau)}\Psi(\tau)\mathrm{d}\tau + \int_0^t \tau e^{t}\Psi(\tau)\mathrm{d}\tau, \quad \Psi(0) = 1, \tag{7.2}$$

where the exact solution is $\Psi(t) = e^{-t}$. After the shock wave, the corresponding V-FIE with phase-lag becomes

$$\begin{aligned}\Psi(t+0.0001) = {} & (t+0.0001) - e^{(t+0.0001)} + e^{-(t+0.0001)} + 1 \\ & + \int_0^1 e^{((t+0.0001)+\tau)}\Psi(\tau)\mathrm{d}\tau + \int_0^{(t+0.0001)} \tau e^{(t+0.0001)}\Psi(\tau)\mathrm{d}\tau.\end{aligned} \tag{7.3}$$

The proposed shifted Legendre least-squares method is applied to this problem for different discretization parameters.

Table 4 reports the absolute errors obtained using the present method and compares them with those reported in [16] for representative values of the time discretization and truncation order.

The numerical results demonstrate that the proposed method achieves significantly smaller errors than the reference method for comparable parameter values. Furthermore, the accuracy improves systematically as the truncation order increases, confirming the convergence and stability of the approach.

Figures 4 and 5 compare the approximate and exact solutions. The numerical solutions obtained by the present method closely match the exact solution over the entire interval, confirming the effectiveness of the shifted Legendre least-squares formulation for phase-lagged Volterra–Fredholm integral equations.

Table 4. Comparison of absolute errors for Example 7.2 obtained using the proposed shifted Legendre least-squares method and the method reported in [16] for different discretization parameters.

t_i	Method in [16] m= 16	Proposed method N = 6	Method in [16] m= 32	Proposed method N = 8
0.0625	4.05145E-04	1.42547E-07	9.93506E-05	3.65872E-09
0.1875	5.20217E-04	2.93354E-06	1.27569E-04	9.52148E-09
0.3125	6.67972E-04	4.12935E-06	1.63802E-04	5.20147E-08
0.4375	8.57692E-04	6.10658E-06	2.10325E-04	8.24531E-08
0.5625	1.10130E-03	6.85215E-06	2.70063E-04	9.23657E-08
0.6875	1.41410E-03	2.58744E-05	3.46768E-04	9.52148E-08
0.8125	1.81573E-03	3.69854E-05	4.45259E-04	5.82367E-07
0.9375	2.00283E-03	4.25876E-05	5.71723E-04	7.23985E-06

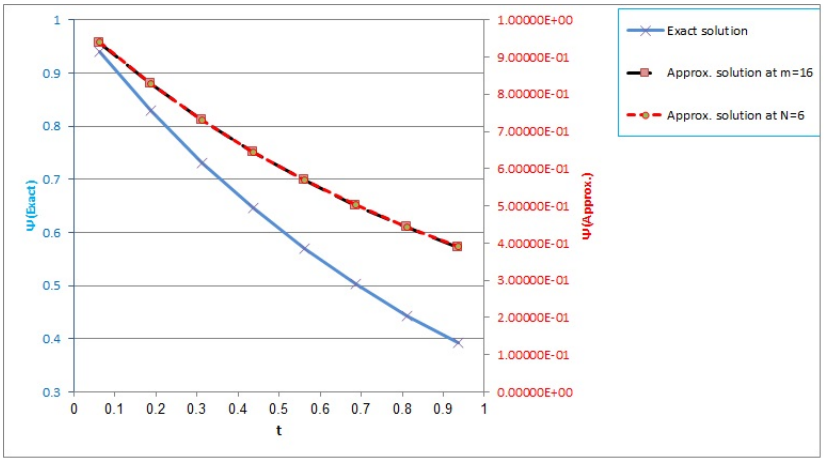

Figure 4. Comparison between the exact solution and the numerical solutions obtained using the method reported in [16] and the proposed method for $m = 16$ and $N = 6$.

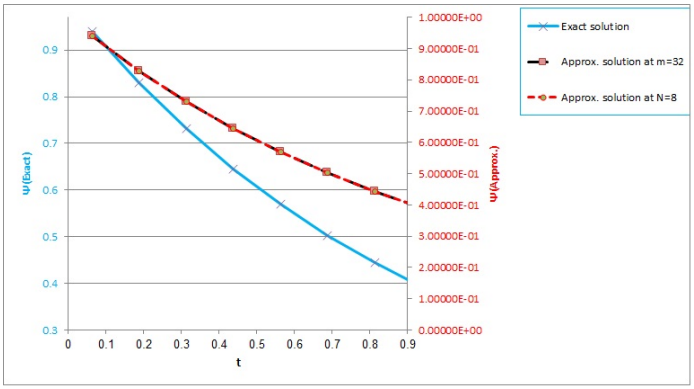

Figure 5. Comparison between the exact solution and the numerical solutions obtained using the method reported in [16] and the proposed method for $m = 32$ and $N = 8$.

Example 7.3. Consider the following V-FIE with a continuous and symmetric kernel:

$$\begin{aligned} 2\Psi(u,t+0.5) = y(u,t+0.5) + \frac{1}{4}\int_0^{t+0.5}\int_0^1 (t+0.5+\tau)|u-v|\Psi(v,\tau)\mathrm{d}v\mathrm{d}\tau \\ + \frac{1}{4}\int_0^{t+0.5}(t+0.5-\tau)\Psi(u,\tau)\mathrm{d}\tau, \quad \Psi(u,0)=0. \end{aligned} \tag{7.4}$$

The exact solution of this problem is given by $\Psi(u,t) = u\ln(1+t)$.

This example is selected to examine the performance of the proposed method in the presence of a continuous and symmetric kernel, which typically leads to smooth solution behavior. The proposed shifted Legendre least-squares method is applied for several time levels $t_m \in [0, 0.4]$ and truncation orders N.

Tables 5–7 report the absolute errors obtained at $t_0 = 0$, $t_1 = 0.2$, and $t_2 = 0.4$, respectively. The numerical results exhibit a systematic reduction in the error as the truncation order N increases, demonstrating the convergence of the proposed approximation scheme. The smoothness induced by the symmetric kernel is effectively captured by the orthogonal shifted Legendre basis, resulting in accurate approximations even for moderate values of N.

Figures 6–8 compare the approximate and exact solutions at representative time levels. The numerical solutions closely coincide with the exact solution over the entire spatial domain $u \in [0, 1]$, and the agreement improves as N increases. These results confirm that the proposed method efficiently exploits kernel regularity and symmetry, yielding stable and accurate numerical solutions for phase-lagged Volterra–Fredholm integral equations.

Table 5. Absolute error for Eq. (7.4) at $t_0 = 0$ for different truncation orders N.

u_i	$N = 3$	$N = 4$	$N = 6$	$N = 10$
0	2.56478E-06	4.69857E-07	1.24757E-07	5.32987E-10
0.1	4.28610E-06	5.36987E-07	2.54321E-07	6.68294E-10
0.2	5.58391E-06	7.52364E-07	4.52876E-07	7.19684E-10
0.3	7.41058E-06	8.23147E-07	5.63217E-07	8.52147E-10
0.4	8.36921E-06	1.23657E-06	7.12548E-07	9.52896E-10
0.5	3.21475E-05	3.69214E-06	9.32564E-07	2.10312E-09
0.6	4.63287E-05	4.96347E-06	9.92548E-07	4.52170E-09
0.7	6.32587E-05	3.65874E-05	3.69254E-06	5.93214E-09
0.8	1.54287E-04	5.20314E-05	5.21369E-06	9.92587E-09
0.9	5.68923E-04	5.72164E-05	5.96328E-06	4.21567E-08
1	6.32187E-04	1.20120E-04	7.52361E-06	5.54269E-08

Table 6. Absolute error for Eq. (7.4) at $t_1 = 0.2$ for different truncation orders N.

u_i	$N = 3$	$N = 4$	$N = 6$	$N = 10$
0	2.93584E-06	6.52387E-07	3.58964E-07	7.63254E-10
0.1	4.92358E-06	8.62394E-07	4.72593E-07	8.76325E-10
0.2	6.72398E-06	8.96325E-07	5.10247E-07	9.53215E-10
0.3	8.23954E-06	9.58236E-07	7.76289E-07	9.85678E-10
0.4	9.16387E-06	2.58694E-06	8.36247E-07	2.56932E-09
0.5	5.36987E-05	4.86322E-06	9.82635E-07	4.75232E-09
0.6	7.52369E-05	5.76328E-06	3.18746E-06	6.93254E-09
0.7	1.58632E-04	6.89520E-05	3.95216E-06	7.82365E-09
0.8	3.69852E-04	9.25847E-05	6.85243E-06	2.56987E-08
0.9	6.92354E-04	9.86254E-05	4.36980E-05	3.25870E-08
1	3.62584E-03	5.38747E-04	5.79632E-05	7.52364E-08

Table 7. Absolute error for Eq. (7.4) at $t_2 = 0.4$ for different truncation orders N.

u_i	$N = 3$	$N = 4$	$N = 6$	$N = 10$
0	3.59247E-06	7.19687E-07	5.87463E-07	8.14627E-10
0.1	5.63891E-06	9.05874E-07	6.24789E-07	9.07854E-10
0.2	7.41308E-06	9.58736E-07	7.74185E-07	9.83674E-10
0.3	9.18387E-06	9.97425E-07	8.57436E-07	2.78615E-09
0.4	9.75632E-06	5.27463E-06	9.38745E-07	3.98762E-09
0.5	9.98326E-05	6.79258E-06	2.57641E-06	5.24781E-09
0.6	2.89647E-04	7.05240E-06	5.74368E-06	8.10421E-09
0.7	3.69287E-04	7.96254E-05	6.58932E-06	3.82147E-08
0.8	4.10739E-04	9.98763E-05	8.46374E-06	4.17258E-08
0.9	7.49634E-04	3.65874E-04	6.30014E-05	5.83691E-08
1	8.28741E-03	5.69874E-04	7.52896E-05	9.23874E-08

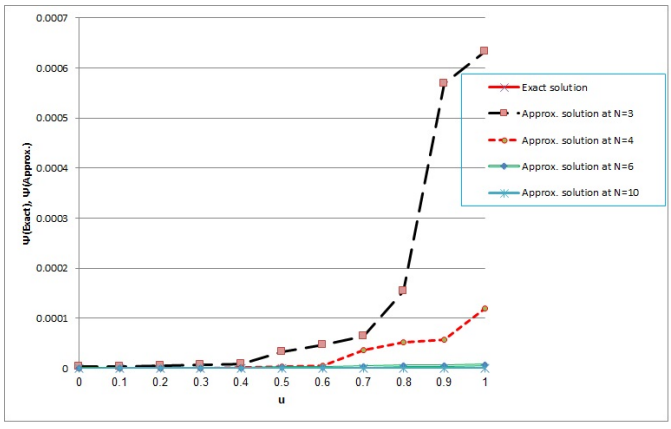

Figure 6. Exact and approximate solutions of Eq. (7.4) at $t_0 = 0$ for different truncation orders N, illustrating the convergence of the proposed method.

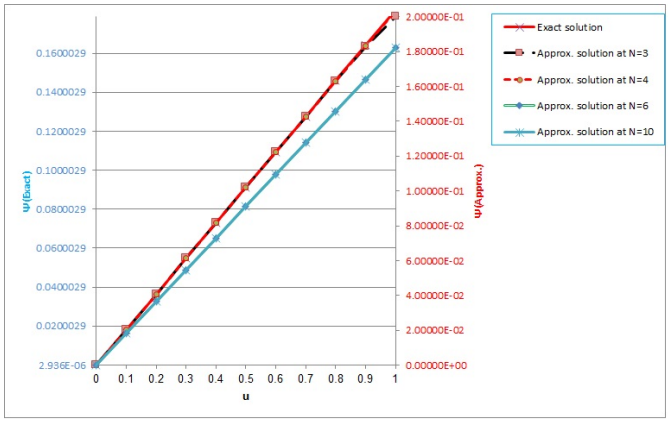

Figure 7. Exact and approximate solutions of Eq. (7.4) at $t_1 = 0.2$ for different truncation orders N, illustrating the convergence of the proposed method.

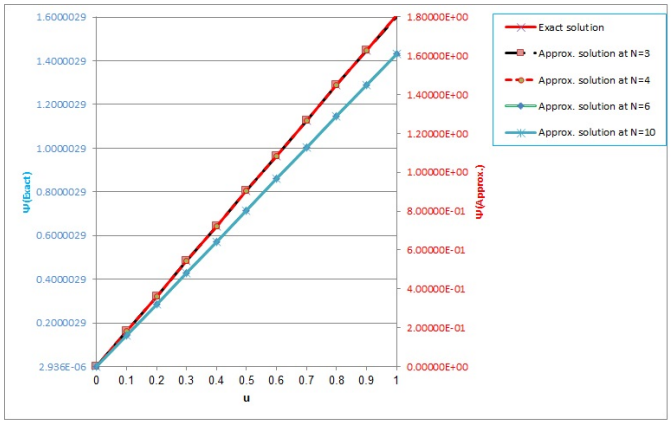

Figure 8. Exact and approximate solutions of Eq. (7.4) at $t_2 = 0.4$ for different truncation orders N, illustrating the convergence of the proposed method.

8. Conclusions

This study proposes a new method for the numerical solution of a class of V-FIE with a phase-lag that arises in problems related to biology and physiology. The process is based on SLPs functions using the LSM. We reduce the problem to an algebraic system by utilizing SLPs as a basis with the LSM and operational matrices of these functions. In comparison with other approaches now in use, the present methodology is easier to build and more accurate. Our claim is supported by the comparison results and the numerical applied models that are described in the research. Numerical experiments (Examples 7.1, 7.3) and comparisons with alternative approaches (Example 7.2) have demonstrated the reliability and efficiency of the suggested method. We conclude that the SLPs method with the LSM is better than the current method in [16] based on the results shown above in Table 4 and Figures 4, 5. According to the numerical results, the current methodology provides reasonable stability, a lower computing workload, and good convergence by increasing N and noting that the accuracy will increase while decreasing the time t. Figures 1–8 and Tables 1–7, which obtain the view, show the simulations of the suggested approaches that were used to get the theoretical results that, which are explained as

follows:

(i) Based on Example 7.1, we can observe from Table 3 that the maximum absolute error occurs when the position is $u = 1$ and the time is $t = 0.6$, the error value at this point is (1.521E-06) at $N = 4$. As we reduce the time and increase N, we can see in Table 1 that the absolute error value begins to decrease until the time reaches 0, this means that the error is increased if the time is increased and N is decreasing.

(ii) From Table 4 in Example 7.2, the numerical results presented in the table clearly demonstrate that the proposed method significantly outperforms the technique of [16] for all tested time levels t_i. In all cases, the absolute errors produced by the presented method are several orders of magnitude smaller than those obtained using the technique of [16]. It is worth noting that the proposed method achieves substantially higher accuracy using fewer discretization parameters (e.g., $N = 6, N = 8$) compared to the method of [16], which requires larger values of ($m = 16, m = 32$). This highlights the efficiency of the proposed approach in reducing computational cost while maintaining superior accuracy. For all values of $t_i \in (0, 1)$, the errors associated with the proposed method remain consistently small and stable, indicating strong numerical stability and robustness of the technique over the entire computational interval.

(iii) From Table 5 in Example 7.3 and decrease the value phase-lag to see its effect, we get the maximum absolute error value is (5.32987E-10) at the position $u = 0$, the time $t = 0$ and $N = 10$. Also from Table 7, we obtain the minimum absolute error value is (8.28741E-04) at the position $u = 1$, the time $t = 0.4$ and $N = 10$, this means that if the values of phase-lag decrease, then the error value is also decreasing.

In future work, we'll discuss the following equation, which has several applications in communication problems and mathematical physics. It can be defined as follows:

$$\eta\Psi(u,t) = y(u,t) + \mu \int_0^t \int_0^1 G(t,\tau)k(u,v)\Psi(v,\tau)\mathrm{d}v\mathrm{d}\tau + \mu \int_0^t U(t,\tau)\Psi(u,\tau)\mathrm{d}\tau, \tag{8.1}$$

considering the dynamic conditions

$$\int_0^1 \Psi(u,t)\mathrm{d}u = P(t), \quad \int_0^1 u\Psi(u,t)\mathrm{d}u = M(t). \tag{8.2}$$

However, in mathematical physics problems, the following given function can be taken into consideration:

$$y(u,t) = \frac{\pi}{\theta_1 + \theta_2}[\gamma(t) + \beta(t)u - h_1(u) - h_2(u)],\ 0 \le u \le 1,\ t \in [0,T],$$
$$\text{and}\ \ \theta_j = \frac{1-\mu_j}{\pi E_j},\ j = 1,\ 2.$$

Acknowledgements

This work was funded by the Deanship of Graduate Studies and Scientific Research at Jouf University under grant No.(DGSSR-2025-02-01388). Also, the authors are very grateful to the editors and referees for their helpful and wonderful comments that led to the development and improvement of our manuscript both scientifically and linguistically.

References

[1] M. A. Abdou, et al., *The error behaviour of collocation and Galerkin methods in solving integral equations*, Benha Journal of Applied Sciences, 2020, 5(7), part (1)-(2), 189–198.

[2] A. Abouelregal, *On Green and Naghdi thermoelasticity model without energy dissipation with higher order time differential and phase-lags*, Journal of Applied and Computational Mechanics, 2020, 6(3), 445–456.

[3] S. A. Abusalim, et al., *An algorithm for the solution of nonlinear Volterra–Fredholm integral equations with a singular kernel*, Fractal Fract, 2023, 7(10), 730.

[4] F. Afiatdoust, et al., *A four-block scheme for nonlinear third-kind Volterra integral equations*, Computational and Applied Mathematics, 2025, 44(7), 1–13.

[5] F. Afiatdoust, et al., *An efficient computational method for nonlinear mixed Volterra–Fredholm integral equations*, Journal of Applied Mathematics and Computing, 2025, 71, 1777–1790.

[6] J. Alahmadi, M. A. Abdou and M. A. Abdel-Aty, *Analytical and numerical treatment of a nonlinear Fredholm integral equation in two dimensions*, J. Appl. Math. Comput., 2024, 70(5), 1–27.

[7] M. A. Abdel–Aty and M. A. Abdou, *Analytical and numerical discussion for the phase-lag Volterra-Fredholm integral equation with singular kernel*, Journal of Applied Analysis & Computation, 2023, 13(6), 3203–3220.

[8] T. Baghban, et al., *A numerical method based on the piecewise Chebyshev cardinal functions for a class of third-kind nonlinear fractional integro-differential equations*, International Journal of Computer Mathematics, 2025, 1–25.

[9] T. Baghban, et al., *A piecewise logarithmic Jacobi cardinal scheme for nonlinear third-kind fractional integro-differential equations*, Applied Numerical Mathematics, 2026, 220, 167–188.

[10] S. Bazm and A. Hosseini, *Bernoulli operational matrix method for the numerical solution of nonlinear two-dimensional Volterra–Fredholm integral equations of Hammerstein type*, Computational and Applied Mathematics, 2020, 39, 1–20.

[11] W. Chew, M. S. Tong and H. U. Bin, *Integral Equation Methods for Electromagnetic and Elastic Waves*, Springer Nature, 2022.

[12] S. M. Abo-Dahab, et al., *Fractional derivative order analysis and temperature-dependent properties on P- and SV-waves reflection under initial stress and three-phase-lag model*, Results in Physics, 2020, 18, 103270.

[13] L. M. Delves and J. L. Mohamed, *Computational Methods for Integral Equations*, Cambridge University Press, 1985.

[14] W. Deng, *Output feedback backstepping control of hydraulic actuators with valve dynamics compensation*, Mechanical Systems and Signal Processing, 2021, 158, 107769.

[15] I. M. Esuabana, U. A. Abasiekwere and I. U. Moffat, *Solution methods for integral equations-a survey*, J. Math. Comput. Sci., 2020, 10(6), 3109–3142.

[16] J. H. He, et al., *Improved block-pulse functions for numerical solution of mixed Volterra-Fredholm integral equations*, Axioms, 2021 10(3), 200.

[17] M. H. Heydari, Z. Avazzadeh and A. Atangana, *Orthonormal shifted discrete Legendre polynomials for solving a coupled system of nonlinear variable-order time fractional reaction-advection-diffusion equations*, Applied Numerical Mathematics, 2021, 161, 425–436.

[18] M. H. Heydari, D. Baleanu and M. Bayram, *Piecewise logarithmic Chebyshev cardinal functions: Application for nonlinear integral equations with a logarithmic singular kernel*, Applied Numerical Mathematics, 2025, 217, 355–371.

[19] M. Holland, et al., *Modeling of induction heating of thermoplastic composites*, Journal of Thermoplastic Composite Materials, 2022, 35(10), 1772–1789.

[20] S. Khan, *Numerical approximation of Volterra integral equations with highly oscillatory kernels*, Results in Applied Mathematics, 2024, 23, 100483.

[21] A. A. Khidir, *A numerical technique for solving Volterra-Fredholm integral equations using Chebyshev spectral method*, Ricerche di Matematica, 2022, 71(2), 1–19.

[22] A. A. Kilany, et al., *Derivative analysis of fractional order on reflection of p-waves with electromagnetic, temperature, and initial stress with three-phase-lag*, Case Studies in Thermal Engineering, 2023, 49, 103325.

[23] A. M. S. Mahdy, et al., *A computational technique for solving three-dimensional mixed volterra–fredholm integral equations*, Fractal and Fractional, 2023, 7(2), 196.

[24] H. M. Malaikah, *The Adomian decomposition method for solving Volterra-Fredholm integral equation using Maple*, Appl. Math., 2020, 11, 779–787.

[25] R. T. Matoog, M. A. Abdou and M. A. Abdel-Aty, *New algorithms for solving nonlinear mixed integral equations*, AIMS Mathematics, 2023, 8(11), 27488–27512.

[26] S. Micula, *Numerical solution of two-dimensional Fredholm–Volterra integral equations of the second kind*, Symmetry, 2021, 13(8), 1326.

[27] F. Mirzaee and N. Samadyar, *Numerical solution of two dimensional stochastic Volterra–Fredholm integral equations via operational matrix method based on hat functions*, SeMA Journal, 2020, 77(3), 227–241.

[28] N. Abdel Mohsen, et al., *A simple iterative approach for some fractional order models of engineering applications*, Benha Journal of Applied Sciences, 2024, 9(5), 89–96.

[29] M. Mozafarifard, *Numerical study of anomalous heat conduction in absorber plate of a solar collector using time-fractional single-phase-lag model*, Case Studies in Thermal Engineering, 2022, 34, 102071.

[30] M. E. Nasr, et al., *A numerical study of nonlinear mixed Volterra-Fredholm integral equations using Toeplitz matrix method*, Journal of Mathematics and Computer Science, 2026, 40(1), 84–100.

[31] S. Nemati, *Numerical solution of Volterra–Fredholm integral equations using Legendre collocation method*, Journal of Computational and Applied Mathematics, 2015, 278, 29–36.

[32] S. K. Panda, T. Abdeljawad and C. Ravichandran, *Novel fixed point approach to Atangana-Baleanu fractional and L_p-Fredholm integral equations*, Alexandria Engineering Journal, 2020, 59(4), 1959–1970.

[33] D. P. Patil, P. D. Shinde and G. K. Tile, *Volterra integral equations of first kind by using Anuj transform*, International Journal of Advances in Engineering and Management, 2022, 4(5), 917–920.

[34] L. Sun, et al., *Shifted Legendre polynomials algorithm used for the numerical analysis of viscoelastic plate with a fractional order model*, Mathematics and Computers in Simulation, 2022, 193, 190–203.

[35] W. Y. Tey, et al., *Moving least squares method and its improvement: A concise review*, Journal of Applied and Computational Mechanics, 2021, 7(2), 883–889.

[36] K. F. Warnick, *Numerical Analysis for Electromagnetic Integral Equations*, Artech House, 2008.

[37] A. Wazwaz, *Linear and Nonlinear Integral Equations: Methods and Applications*, Springer: Berlin, Heidelberg, Germany, 2011.

[38] A. M. Wazwaz, *Linear and Nonlinear Integral Equations: Methods and Applications*, Springer, New York, USA, 2011.

Received July 2025; Accepted May 2026; Available online June 2026.